INSTITUTE OF PHYSICS PUBLISHING NONLINEARITY

Nonlinearity **15** (2002) 45–64 PII: S0951-7715(02)18303-4

Many-body symbolic dynamics of a classical oscillator chain

Marko Žnidarič and Tomaž Prosen

Physics Department, Faculty of Mathematics and Physics, University of Ljubljana, Jadranska 19,1111 Ljubljana, Slovenia

E-mail: znidaricm@fiz.uni-lj.si and prosen@fiz.uni-lj.si

Received 25 October 2000, in final form 13 September 2001
Published 26 November 2001
Online at stacks.iop.org/Non/15/45

Recommended by P Gaspard

Abstract

We study a certain type of the celebrated Fermi–Pasta–Ulam particle chain, namely the inverted FPU model, where the interparticle potential has the form of a quartic double well. Numerical evidence is given in support of a simple symbolic description of dynamics (in the regime of sufficiently high potential barrier between the wells) in terms of an (approximate) Markov process. The corresponding transition matrix is formally identical to a ferromagnetic Heisenberg quantum spin-1/2 chain with long-range coupling, whose diagonalization yields accurate estimates for a class of time correlation functions of the model.

PACS number: 0545

1. Introduction

In a historical numerical experiment, Fermi, Pasta and Ulam [1] studied the following non-linear model of a one-dimensional crystal described by the Hamiltonian

$$H = \sum_{i=1}^{N} \left(\tfrac{1}{2} m \dot{x}_i^2 + V(x_i - x_{i-1} - l) \right), \qquad V(x) = \tfrac{1}{2} m\omega^2 x^2 + \tfrac{1}{4} k x^4. \tag{1}$$

Contrary to the initial expectations of Fermi *et al*, the so-called FPU model (1) behaved in strong contrast to the ergodic theorem of statistical mechanics, even in a quite strongly non-linear regime when one would expect fast relaxation to statistical canonical equilibrium and equipartition of energy from an arbitrary initial state. Instead, the FPU model triggered the discovery of non-linear normal modes, the so-called *solitons*, and indirectly, the whole field of (computational) non-linear dynamics. Later, the FPU chain was studied in the spirit of the KAM theory [2] and various estimates have been given for the critical strength of the

dimensionless non-linearity parameter $kl^2/m\omega^2$ required for the motion to become globally stochastic [3, 4].

Recently, FPU-type models have been studied in the context of energy transport and Fourier heat law in one-dimensional chains of particles [5–7]. Quite unexpectedly, FPU-type models, namely Hamiltonians of the type (1) with non-linear interparticle interaction $V(x)$ (and no *on-site* potential), turned out to be anomalous heat conductors, due to slow power-law decay of transport (velocity–velocity or current–current) time correlation functions. These results, namely that correlations decay universally as $C(t) \sim t^{-3/5}$, and correspondingly that the Kubo transport coefficient diverges as $\kappa(L) \sim L^{2/5}$ as a function of the chain length L, were later successfully explained in terms of hydrodynamic arguments and mode–mode coupling theory [8].

However, a perturbative-like approach such as mode–mode coupling theory should break down when the interparticle potential has *more than one* stable position. Indeed, Giardina *et al* [9] have performed a series of numerical experiments on the particle chain with an oscillating interparticle potential $V(x) = 1 - \cos(x)$, as well as with the potential $V(x) = -x^2/2 + x^4/4$, and found normal heat conduction with a clean exponential decay of correlations. On the other hand, it has been shown in [10] that the Kubo expression for thermal conductivity of momentum-conserving systems diverges provided the equilibrium pressure is non-vanishing. This result does not contradict the findings of [9] as the equilibrium pressure of their model is zero. The key mechanism, which we believe produces non-KAM-like (almost) hyperbolic motion of such a high-dimensional Hamiltonian system, are the hyperbolic saddles over which pairs of particles flip from one well to another. Additionally, the size of elliptic regions is expected to decay fast with the size of the system [11]. Thus, the system will behave effectively as Anosov-like [12]. This motivated us to study, in this paper, some fundamental dynamical properties of the simplest version of such a hyperbolic chain with quartic double-well interparticle potential $V(x)$. We present here some intriguing numerical results which suggest the existence of a simple (but only approximate) Markov partition with very simple many-body symbolic dynamics of this particle chain. In addition, we find that the transition matrix is formally generated by a Hamiltonian of a certain quantum spin-1/2 chain.

Section 2 introduces the model. In section 3, we define the (approximate Markov) partition of phase space and obtain numerical and analytical estimates for the volumes of various cells. An expression for the average time between subsequent jumps among the cells is also obtained. In section 4, we introduce a Markovian description of our model with the transition matrix and the flux matrix, and numerically check the accuracy of the Markovian property in two independent ways. Section 5 represents the core of the present paper. We numerically calculate the transition matrix and make a formal correspondence between our model and a ferromagnetic Heisenberg quantum spin-1/2 chain. Using this correspondence, we derive various estimates and bounds for the decay rates of the time correlation functions of a class of piecewise constant functions.

2. Model: inverted Fermi–Pasta–Ulam chain

With the choice for units of mass, time and length of m, $1/\omega$ and l, respectively, and the new canonical coordinates $q_i = x_i - il$ and $p_i = m\dot{x}_i$, Hamiltonian (1) can be brought to a dimensionless form,

$$H = \sum_{i=1}^{N} \frac{p_i^2}{2} + V(q_i - q_{i-1}), \qquad V(x) = -\alpha\frac{x^2}{2} + \frac{x^4}{4} + \frac{\alpha^2}{4}, \tag{2}$$

where $\alpha = -m\omega^2/kl^2$ is the only dimensionless parameter left (see figure 1). In order for the potential minima to be at level 0 (for $\alpha > 0$), we have added a constant term $\alpha^2/4$ to

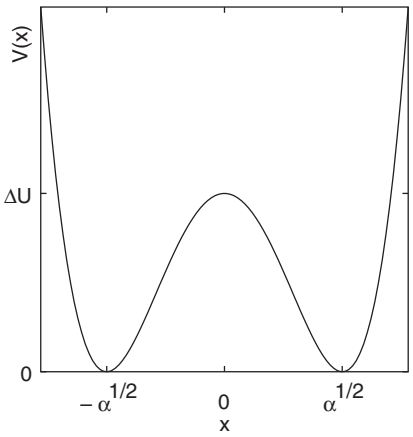

Figure 1. Potential $V(x)$ for the inverted FPU model (2), $\alpha > 0$.

the potential $V(x)$. We can obtain different orbits of the system described by the Hamilton function (2) by varying only one parameter α. At first, it would seem that the energy E is also a free parameter. But, by fixing all three basic units, we have also provided a natural unit for the energy density $\varepsilon = E/N$. If we scale the dimensionless quantities by a factor ξ, namely $(q_i, p_i, \alpha) \rightarrow (\xi q_i, \xi^2 p_i, \xi^2 \alpha)$, the Hamiltonian is simply multiplied by a factor ξ^4. The invariant parameter in this transformation is, therefore, $\lambda = \varepsilon/\alpha^2$. All different non-equivalent Hamiltonians can be obtained just by varying one parameter, namely λ, or equivalently α at fixed ε. The energy density can, therefore, be fixed without any loss of generality. From now on, $\varepsilon = E/N = 1$ is assumed, as well as periodic boundary conditions $(q_{N+1}, p_{N+1}) \equiv (q_1, p_1)$. A phase space point will be denoted by $\boldsymbol{x} = (\boldsymbol{q}, \boldsymbol{p})$. For negative values of the parameter α, the system has the form of the standard β-FPU model (just in a different parametrization), but in this paper we focus on the positive values of the parameter α in which case we call the system the *inverted FPU model* (IFPU). The IFPU model is translationally invariant; therefore, besides the energy ε there is also a second (trivial) constant of motion, namely the total momentum $P = \sum_{i=1}^{N} p_i$. In all numerical calculations the total momentum has been fixed to $P = 0$.

For the numerical integration of equations of motion, a fourth-order symplectic algorithm of [13] has been used. This integrator has been checked to be the optimal choice (at least for the model studied here, and at relative accuracy $\sim 10^{-5}$–10^{-8}) by making a careful comparison with a number of other symplectic and Runge–Kutta methods.

3. Phase space partition and statistical dynamics

If the barrier $\Delta U = \alpha^2/4$ between the potential minima is sufficiently high, the differences $(q_{i+1}(t) - q_i(t))$ will spend most of the time either around the left or the right minimum with quite infrequent jumps between the wells. As the motion around the minimum is approximately harmonic, the more interesting part will be the transitions between the left and the right potential well, for each pair of neighbouring particles, going over the hyperbolic saddle at $q_{i+1} - q_i = 0$. Understanding the motion in phase space of a high-dimensional system is generally very difficult. Therefore, some symbolic description of an orbit $\boldsymbol{x}(t)$ is highly desirable. In the IFPU model with high potential barrier, the choice of a partition of phase space is almost obvious.

For each instant of time t we will be interested only in a single binary bit of information $a_i \in \{0, 1\}$ for each pair of neighbouring particles $(i, i + 1)$, namely if the neighbours are in

the right or left well, $(q_{i+1} - q_i) > 0$ or < 0, we write $a_i = 1$ or $a_i = 0$, respectively. Binary positions for the whole chain can be compactly encoded in a binary integer (*signature*):

$$S = (a_N \dots a_2 a_1)_2 = \sum_{i=1}^{N} a_i 2^{i-1}. \tag{3}$$

Thus, we have defined a partition of $2N$-dimensional phase space cut by N hyper-planes $q_{i+1} = q_i$ into 2^N cells labelled by signatures $S \in \{0, 1, \dots, 2^N - 1\}$. By a slight abuse of language, we will use the term *signature* S also to refer to a phase space cell denoted by S. If the transitions between various signatures are rare, which is obviously the case if the potential barrier ΔU is high, it seems to be meaningful to concentrate on the (statistical) dynamics of transitions between the signatures. For the periodic boundary conditions the coordinate differences must fulfil the constraint $\sum_{i=1}^{N} (q_{i+1} - q_i) \equiv 0$, which, in the limit of infinitely high potential barrier and even N, translates into the condition $\sum_{i=1}^{N} a_i = N/2$. For odd N the number of pairs in the left and the right wells should differ by 1. This presents unnecessary technical complications and, from now on, we will assume N to be even. If the barrier is finite, signatures with different numbers of pairs in the left and right well are possible to visit. We will call signature S of order i if $\sum_{i=1}^{N} a_i = N/2 \pm i$. The number of different signatures M_i of order i is

$$M_i = \binom{N}{N/2 - i} = \frac{N!}{(N/2 - i)!(N/2 + i)!}. \tag{4}$$

For a sufficiently high barrier, the system will spend most of its time in signatures of order 0. We will specifically concentrate on signatures of order 0 and treat signatures of higher (mostly first) order only as 'tunnels' for transitions between different signatures of order 0. Figure 2 shows an example of a transition between two order 0 signatures via an intermediate short-lived signature of order 1. First, we have to know for which values of parameter α and size N will the description by the signatures of order 0 alone be adequate, i.e. will the relative time spent in higher-order signatures be negligible.

3.1. Estimating the fractional volumes of higher-order signatures

We will now make a rough theoretical estimate for the time spent in signatures of different orders. For an ergodic system, this time is proportional to the measure (volume) of the phase space covered with the signatures in question. Let us designate by t_i the time spent in signatures of order i. We have

$$t_i(E) \propto \int_{\text{order } i} \frac{\mathrm{d}S}{|\nabla H|} = \frac{\mathrm{d}\Gamma_i(E)}{\mathrm{d}E}, \tag{5}$$

where the region of integration is the part of the energy surface $H = E$ intersecting with the full set of signatures of order i, and $\Gamma_i(E)$ is the total volume of the phase space in the signatures of order i and with energy less than E. First, let us make an estimate for $\Gamma_0(E)$. The potential around both minima is to the lowest-order harmonic; therefore, we can roughly say $\Gamma_0(E) \approx \Gamma(E)^N$, where $\Gamma(E)$ is the volume for one harmonic oscillator, that is $\Gamma(E) = 2\pi E/\sqrt{\alpha}$. For the signatures of order i, the argument is very similar. In this case, there are $2i$ particles more in one potential well than in the other. Because the trivial condition $\sum_{i=1}^{N} (q_{i+1} - q_i) \equiv 0$ must still be satisfied, the equilibrium positions of pairs will not be at $\pm\sqrt{\alpha}$ any more but will be shifted for Δq in order to keep the centre of mass of all pairs at 0. This gives the shift as $\Delta q = 2i\sqrt{\alpha}/N$, and contributes $\varepsilon_i = \alpha \Delta q^2 = 4i^2\alpha^2/N^2$ to the energy density, provided the cubic part of the potential is negligible, i.e. $2i/N \ll 1$. The harmonic approximation for the volume $\Gamma_i(E)$ can therefore still be used, but now at energy $E - N\varepsilon_i$.

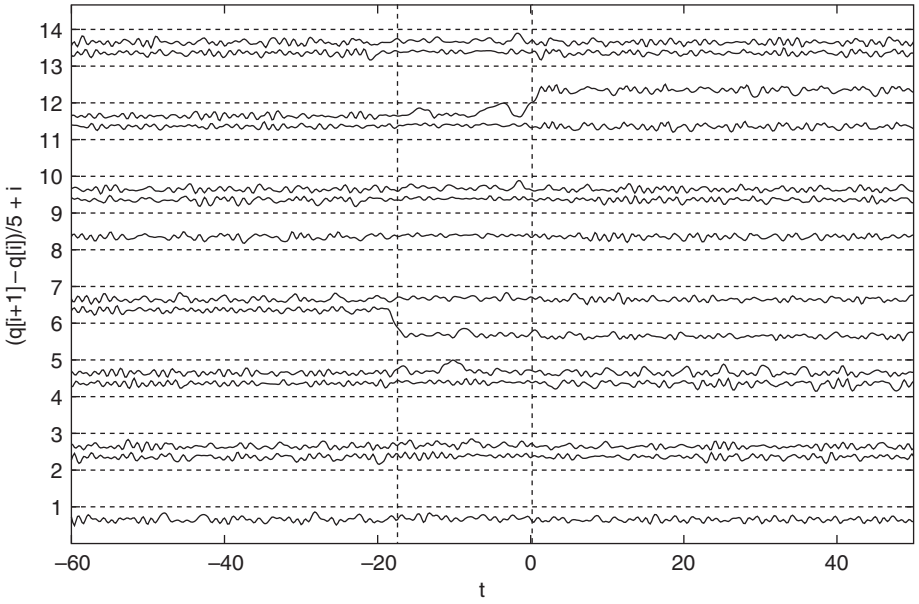

Figure 2. Time dependence of differences $(q_{i+1}(t) - q_i(t))$ for $N = 14, \alpha = 4.8$. For time $t < -20$, the system is in the order 0 state $S = 01010110101010_2$, at $t \approx -20$ the system jumps to the temporary order 1 metastable state $S'' = 01010110001010_2$ and shortly thereafter at $t = 0$ jumps into the new stable order 0 state $S' = 01110110001010_2$. Such a transition from S to S' will be called a jump of length $d = 6$. Dashed lines denote the position of the saddles $q_{i+1} = q_i$.

Since we are interested only in the dependence for large N we can omit ('cancel') energy derivatives coming from (5), so that we have

$$\frac{t_i}{t_0} \sim \frac{\Gamma(\varepsilon - \varepsilon_i)^N}{\Gamma(\varepsilon)^N} = \left(1 - \frac{\varepsilon_i}{\varepsilon}\right)^N \sim \exp\left(-4i^2 \frac{\alpha^2}{N\varepsilon}\right). \tag{6}$$

We have fixed $\varepsilon \equiv 1$ so that the relative fraction of signatures of order 1, t_1/t_0, falls exponentially in α^2/N. We must stress that the exponential dependence is expected only when $4\alpha^2/N^2 \ll 1$ and that the overall prefactor in front of an exponential function could still depend on N. This is well confirmed by the numerical data in figure 3. Grouping the signatures by their order is meaningful since members of each group have the same phase space volume and the same minimal potential energy. The minimal potential energy of order 0 signatures is $\varepsilon_0 = 0$, of order 1 is $\varepsilon_1 = 4\alpha^2/N^2$, and of order i is $\varepsilon_i \approx i^2\varepsilon_1$. The fraction of time spent in higher-order signatures is just a power of the relative time spent in order 1 signatures, $(t_i/t_0) \approx (t_1/t_0)^{i^2}$ and this can be reduced by increasing α.

Of course, for the transitions to be possible at all, the barrier height must be smaller than the total energy E. This yields the condition

$$\alpha^2/4 < N, \tag{7}$$

which is just the opposite of the condition to keep t_1/t_0 small. Nevertheless, we can still reduce the fraction of higher-order states sufficiently. But the condition (7) can be problematic for small N. Indeed, for the smallest non-trivial case of $N = 4$ we have numerically found that there are no transitions between signatures for $\alpha \geqslant 2.8$. For smaller α we do find transitions, but there the system exhibits non-ergodic behaviour. The condition (7), although fulfilled, seems to be too weak and is still keeping the phase space cut into non-connected parts. The smallest system worth studying regarding transitions is therefore $N = 6$.

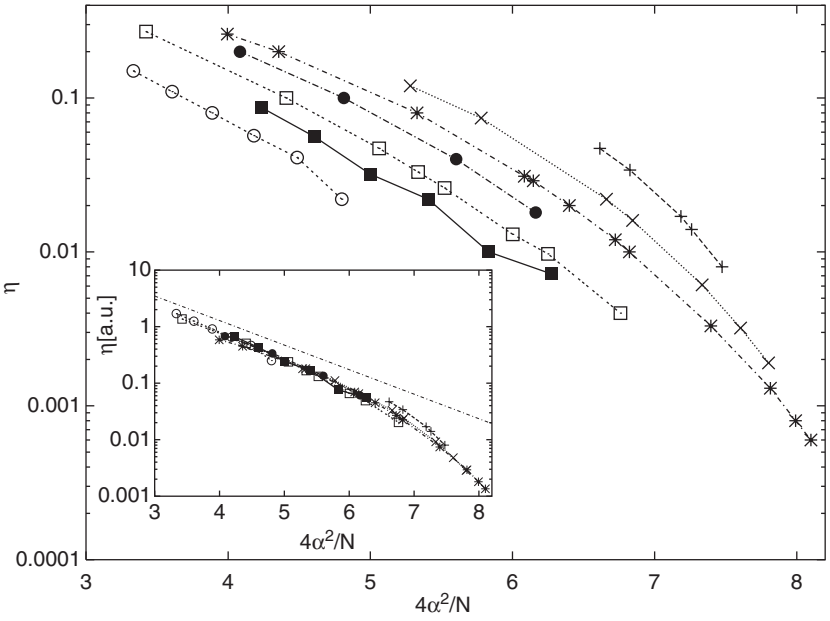

Figure 3. Fraction $\eta = (\sum_{i=1}^{\infty} t_i)/t_0 \approx t_1/t_0$ of time spent in signatures of higher order for $N = 6, 8, 10, 12, 16, 20$ and 30, from right to left, respectively. Lines connect points with the same value of N. The inset shows by the N-dependent prefactors the rescaled values of η and exponential function (6) (chain straight line).

In all numerical work, α and N have been chosen so as to keep the fractional volume of higher-order signatures small. We have, therefore, studied the dynamics on a set of M_0 signatures of order 0 exhibiting transitions through short-lived order 1 signatures as shown in figure 2. The most important physical scale that characterizes such a transport is the average time τ between subsequent transitions.

3.2. Ergodicity and the average transition time τ between signatures of order 0

Though the main body of this paper is concerned with the transport and decay of time-correlations, i.e. with the system's mixing property, we should first mention, that we have also checked the weaker dynamical property of ergodicity directly. We have employed the method of Robnik *et al* [14] of comparing the rate of visiting of different phase space cells (in our case, order 0 signatures) with the rate for a fully random dynamics. The results turned out to be fully consistent with (uniformly) ergodic behaviour of our IFPU model in the high-barrier regime discussed above.

Now we define the timescale τ to be an average time from the point when the orbit enters a certain order 0 signature S to the point where the same orbit enters the next order 0 signature S' ($S' \neq S$) concluding the transition from S to S'. The average is taken over many different orbits with microcanonically distributed initial conditions, or over one very long orbit if we assume ergodicity. We obtain an approximate functional form for the dependence of τ on N and α by similar arguments as for the relative volume of higher-order signatures. The probability for a jump will be estimated by the ratio between the phase space volume of the set of states just before a jump Γ_t and the volume of the set of equilibrium states Γ_{eq}. The approximate volume $\Gamma_{eq}(E)$ of the phase space of equilibrium states has been derived in the previous subsection

and is given as $\Gamma_{\rm eq}(E) \approx \Gamma(E)^N = (2\pi/\sqrt{\alpha})^N E^N$. In the state just before the transitions, there should be more than ΔU of energy in one pair of particles. This energy will be denoted by $a\alpha^2$, where a is, for now, some unspecified constant. Certainly, a must be greater than $1/4$; but, because our oscillators are coupled, we allow for the possibility that the energy of a pair must actually be bigger than the barrier height. The phase volume $\Gamma_{\rm t}(E)$ for a state with one pair having the energy $a\alpha^2$ and the other $N-1$ pairs residing in the minima is

$$\Gamma_{\rm t}(E) = \int_0^{E-a\alpha^2} {\rm d}\varepsilon\, \varepsilon^{N-2} \left(\frac{2\pi}{\sqrt{\alpha}}\right)^{N-1} \{(N-1)\Gamma(E) - N\Gamma(\varepsilon)\}$$
$$= \left(\frac{2\pi}{\sqrt{\alpha}}\right)^N a\alpha^2 (E - a\alpha^2)^{N-1}. \tag{8}$$

The probability for a jump is proportional to the quotient of derivatives ${\rm d}\Gamma_{\rm t}(E)/{\rm d}\Gamma_{\rm eq}(E)$. The reciprocal average time between transitions $1/\tau(N,\alpha)$ is proportional to the above quotient and to the frequency of oscillation around the potential minimum. Using also $E = N$, we finally get

$$\tau(N,\alpha) \approx \frac{A}{\sqrt{\alpha}} \frac{N}{a\alpha^2} \frac{1}{(1 - a\alpha^2/N)^{N-2}}, \tag{9}$$

where A is some overall numerical factor. We have determined the numerical parameters a and A by fitting the numerical data for different lengths N in the range $N = 6, \ldots, 30$ (figure 4). Both parameters depend on N for small chains, but are, of course, independent of α. The value of A is between 0.02 and 0.10, where the a has dependence $a = 1/4 + O(1/N)$. In the limit of large chains, a has the value $1/4$ predicted by our simple physical picture. This picture can also be confirmed by looking at the local energy density just before the jump. Indeed, the local energy of a pair is exactly $a\alpha^2$ for all chain sizes. So, the parameter a is not just some fitting parameter in equation (9) but it has a clear physical interpretation. An interesting scaling law is also worth noticing, although it is only approximate. The dependence of $\tau(N,\alpha)$ is such that we can write, approximately,

$$\tau(N,\alpha) \approx \frac{f(4N/\alpha^2)}{\sqrt{\alpha}} \exp(\alpha^2/4), \tag{10}$$

where $f(x)$ is some parameter-free function. The shape of this function can be seen in figure 5. Note that the data shown are for relatively small chain sizes and the conclusion $f(x) \propto x$, derived from equation (9), is not justified.

We have also numerically computed the statistical distribution of transition times τ_n, i.e. the time intervals between entering different subsequent signatures of order 0 such that $\tau = \langle \tau_n \rangle$, for a fixed N and α. This distribution is shown in figure 6 and is clearly seen to be exponential. There is a discrepancy only for extremely small times. This is a consequence of the duration of intermediate unstable order 1 state that occurs between order 0 states (see figure 2). The fraction of the order 1 state was, in this case, $t_1/t_0 = 0.0013$, which is the same as the timescale of the discrepancy in the figure. Our distribution should be a convolution of distributions of t_0 and t_1. But the precise explanation of this discrepancy is the following: we obtain too many 'short' jumps because of the way we measure the time when the system has arrived in a new order 0 signature. We mark the system as arriving in a new signature exactly at the top of the barrier, when the difference $(q_{i+1} - q_i)$ changes the sign and not when it relaxes to the bottom of the well. This allows for some 'fake transitions' in the regions of phase space where two or more order 0 signatures almost touch with a saddle-like region in between (for instance, near the coordinate origin $q_i \equiv 0$). There it is possible that the system, which although it gets over the barrier, subsequently relaxes into some nearby well because it does not have the 'right' momentum vector.

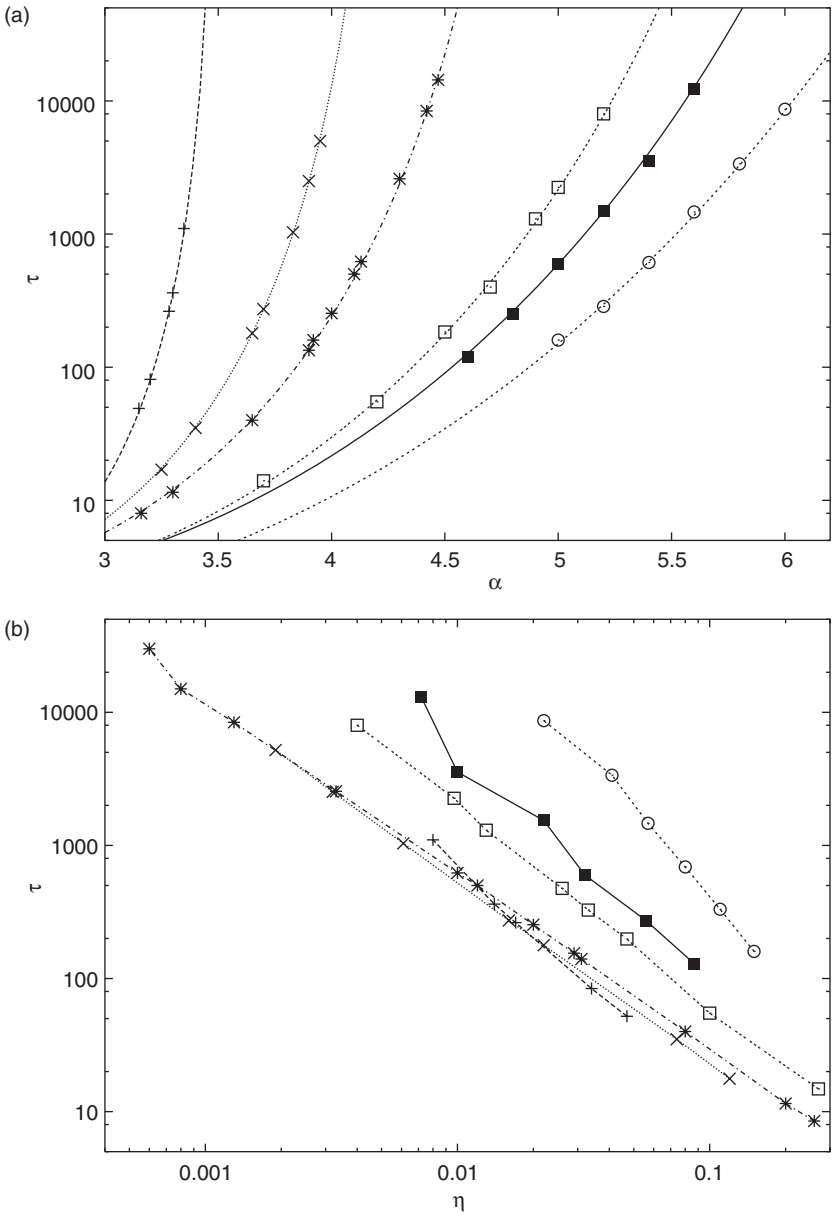

Figure 4. In (*a*), the experimental values of τ for $N = 6, 8, 10, 16, 20$ and 30 (symbols from left to right) and semi-theoretical estimate (with continuous curves) for τ (9) are drawn. Errors in numerical τ are of the same order as the symbol sizes. In (*b*), we plot the dependence of τ on $\eta = (\sum_{i=1}^{\infty} t_i)/t_0$. The data and the symbols used are the same as in (*a*), while the straight line segments here merely connect the points with the same value of N.

4. The Markov process and its transition matrix

We decided to describe the dynamics with a sequence of binary signatures instead of a full orbit $x(t)$ with the hope of some simplification. We are hence looking for some simple statistical

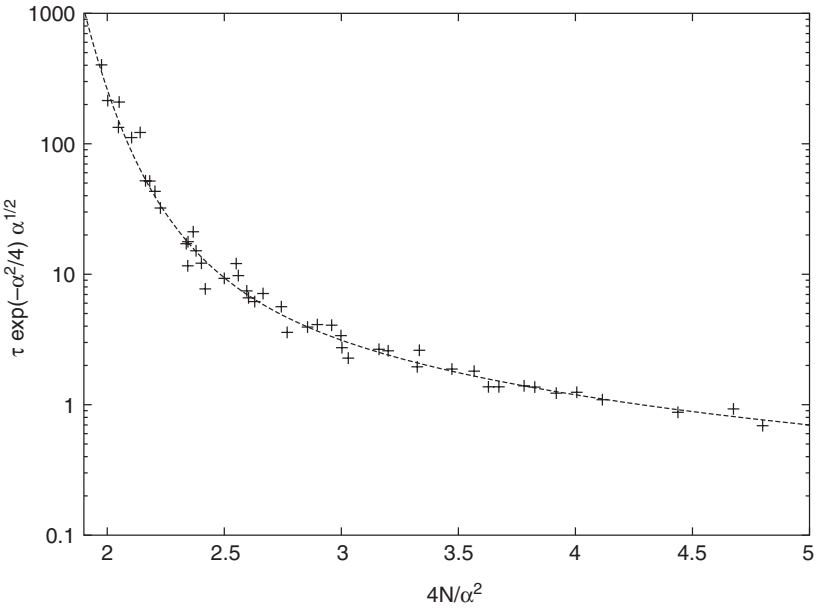

Figure 5. Numerical data for $\tau(N, \alpha)$ divided by $\exp(\alpha^2/4)/\sqrt{\alpha}$ versus $4N/\alpha^2$. The solid curve is only drawn to guide the eye, perhaps suggesting some universal scaling function. The same data as in figure 4.

description of the transitions between signatures. The stochastic system is fully described by giving conditional transition probabilities $P(S, S', S'', \ldots; t, t', \ldots)$. The simplest kind of stochastic process is called a Markov process. For a Markov process, the conditional probabilities $P(S, S'; t)$, to be in a state S' at time t provided we were in S at $t = 0$, contain all the information about the system. For a homogeneous Markov process, these can be defined as

$$P(S, S'; t) = \frac{\langle \delta_{S',S(t'+t)} \delta_{S,S(t')} \rangle_{t'}}{\langle \delta_{S,S(t')} \rangle_{t'}}, \tag{11}$$

where the brackets $\langle\ \rangle_{t'}$ denote a time average over a long orbit (assuming ergodicity) and $\delta_{S,S(t)}$ has value 1 if the orbit is in a signature S at time t, and 0 otherwise. We will write a matrix $P(S, S'; t)$ as just $\boldsymbol{P}(t)$. For now, let us define $P(S, S'; t)$ on the full space of 2^N signatures, although we will later be interested only in transition probabilities among M_0 signatures of order 0. The transition matrix $\boldsymbol{P}$ must satisfy the semigroup condition

$$\boldsymbol{P}(t + t') = \boldsymbol{P}(t)\boldsymbol{P}(t'). \tag{12}$$

Therefore, the matrix $\boldsymbol{P}(t)$ contains some redundant information. We can, instead, write

$$\boldsymbol{P}(t) = \exp(\boldsymbol{F}t), \tag{13}$$

where for a Markov process the matrix $\boldsymbol{F}$ is time independent. The matrix element $F(S, S')$ is a probability flux from the signature S to the signature S', and can be defined by the limit

$$\boldsymbol{F} = \lim_{t \to 0} \frac{\boldsymbol{P}(t) - \boldsymbol{I}}{t}. \tag{14}$$

The conservation of probability imposes the condition $\sum_{S'} F(S, S') = 0$ for the matrix elements.

By a statistical description, using $\boldsymbol{P}(t)$ instead of $\boldsymbol{x}(t)$, we lose information about the details within a single cell of a partition. In other words, we study the dynamics on the space

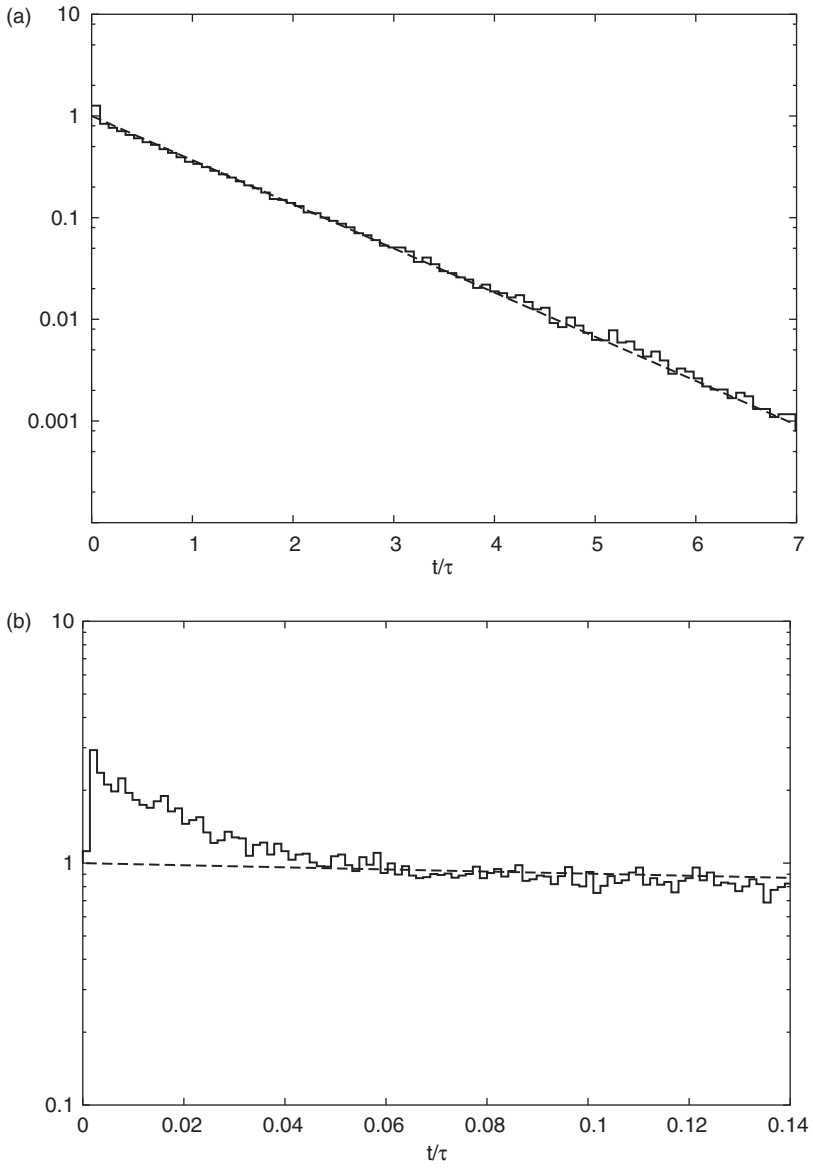

Figure 6. Probability distribution of times $t = \tau_n$ (on a relative scale t/τ) between two different consecutive order 0 signatures. In (*b*), we plot the enlarged distribution for small times. All is for the chain of length $N = 20$ and $\alpha = 5.4$ corresponding to $\tau = 3500$. The dashed line is an exponential function.

of functions that are constant over one phase space cell. This can be formalized by introducing characteristic functions $B_S(\boldsymbol{x})$ over signatures S,

$$B_S(\boldsymbol{x}) = \begin{cases} 1, & \boldsymbol{x} \in S, \\ 0 & \text{otherwise} \end{cases}. \tag{15}$$

The characteristic functions B_S span the space of all observables which are piecewise constant over the signatures. Every piecewise constant observable $W(\boldsymbol{x})$ can be expanded over the base

functions B_S as $W(\boldsymbol{x}) = \sum_S w_S B_S(\boldsymbol{x})$, with the expansion coefficients w_S given by

$$w_S(t) = \frac{\langle B_S W(t)\rangle_E}{\langle B_S\rangle_E}, \tag{16}$$

where the brackets $\langle\ \rangle_E$ denote a microcanonical phase space average over the energy surface $H = E$. The matrix elements of a transition matrix $\boldsymbol{P}$ are nothing but the correlation functions between the characteristic functions

$$P(S, S'; t) = \langle B_{S'}(t) B_S\rangle_E / \langle B_S\rangle_E. \tag{17}$$

As the transition matrix propagates the probabilities between the signatures, we can write the time-dependent vector $\boldsymbol{w}(t) = (w_S(t), w_{S'}(t), \ldots)$ as

$$\boldsymbol{w}(t) = \boldsymbol{P}(t)\boldsymbol{w}(0) = \exp(\boldsymbol{F}t)\boldsymbol{w}(0). \tag{18}$$

Similarly, the autocorrelation function of the observable W is

$$\langle W(t)W(0)\rangle_E = \boldsymbol{w}^{\mathrm{T}}\ \exp(\boldsymbol{F}t)\boldsymbol{w}. \tag{19}$$

We can see that the behaviour of correlation functions is determined by the spectrum of the (Markov) propagator $\exp(\boldsymbol{F}t)$.

From now on we assume that the fraction of higher-order signatures is very small, $\eta \approx t_1/t_0 \ll 1$, and we restrict the matrices $\boldsymbol{P}(t)$ and $\boldsymbol{F}$ on the M_0-dimensional subspace of signatures of order 0, which essentially contain all non-vanishing matrix elements. Numerically, we have calculated the transition matrix $\boldsymbol{P}(t)$ by using definition (11). For small t the average can be performed, and by using expression (14), yields for $F(S, S')$, $(S \neq S')$

$$F(S, S') = \frac{n(S, S')}{t_S}, \tag{20}$$

where $n(S, S')$ is the number of direct transitions between the order 0 signatures S and S', and t_S is the total time spent in the signature S. Here a small comment regarding higher-order signatures is in order. We saw in figure 2 that between each order 0 states there is a short intermediate order 1 state of duration $\sim \tau t_1/t_0$. So there are no direct transitions between order 0 states, and all fluxes $F(S, S')$ (20) among M_0 order 0 signatures are strictly zero. As we have decided to study only (indirect) transitions between order 0 states (for the parameter values where the fraction of higher-order states is negligible) we must somehow circumvent this difficulty. One solution is to calculate the derivative of the transition matrix $\boldsymbol{P}(t)$ in equation (14), not at time $t = 0$ but at time t, with $\tau t_1/t_0 \ll t \ll \tau$. In this case the number $n(S, S')$ in (20) is the number of jumps between order 0 states S and S' with one short intermediate order 1 state. A still more simple and convenient solution is to replace the orbit $\boldsymbol{x}(t)$ by a sequence of times t_i when the orbit hits the boundary of a cell of order 0 coming from outside. Orbit $\boldsymbol{x}(t)$ is, therefore, replaced by a sequence of pairs $\ldots, (S_i, t_i), (S_{i+1}, t_{i+1}), \ldots$ which shows us that at time t_i orbit $\boldsymbol{x}(t)$ came to the order 0 signature S_i, then until time t_{i+1} was in signature S_i or any higher-order signature, and at time t_{i+1} arrived at the next order 0 signature S_{i+1} $(S_{i+1} \neq S_i)$, etc. Then we define $n(S, S')$ as the number of subsequent pairs (S, S') in the sequence $\{S_i\}$, and $t_S = \sum_i^{S_i=S}(t_{i+1} - t_i)$; hence, the flux matrix is calculated as

$$F(S, S') = \frac{\sum_i^{(S,S')=(S_i,S_{i+1})} 1}{\sum_i^{S_i=S}(t_{i+1} - t_i)}. \tag{21}$$

This definition is used in the numerical calculation of this paper.

4.1. Tests for the Markov process

Before describing the process of transitions as Markovian, we must check if this is at all permissible. Checking the rigorous conditions for the partition to signatures to be Markovian, see e.g. [15], is a considerable mathematical problem, at least in our judgement. On the other hand, heuristic arguments and numerical results support the idea that, for sufficiently large transition times τ, the process will indeed be Markovian. The system has positive Lyapunov exponents.[1] Vaguely, this means that the system quickly 'forgets' its history. If the average time between the jumps τ is longer than the Lyapunov time, we can expect the transitions to be Markovian.

Standard tests of Markovian property use the information theoretic approach, e.g. discretizing dynamics in time and then employing a mutual information test. However, for our system this approach has two disadvantages. First, it involves looking at all triples of successive signatures, which is numerically very time-consuming for large τ. And second, we lose the dynamical aspect of the time evolution, i.e. explicit time dependence of transition probabilities $\boldsymbol{P}(t)$. We have, therefore, used several other tests. The most straightforward one is to explicitly check the composition formula (12).

The condition $\boldsymbol{P}(2t) = \boldsymbol{P}^2(t)$ is trivially fulfilled for small and for large times t, $t \ll \tau$ and $t \gg \tau$, respectively. We checked it for time $t = \tau$ by calculating the quantity

$$\sigma = \frac{||\boldsymbol{P}(2\tau) - \boldsymbol{P}^2(\tau)||_{\mathrm{E}}}{||\boldsymbol{P}(2\tau)||_{\mathrm{E}}}, \tag{22}$$

where $||\boldsymbol{A}||_{\mathrm{E}} = (\sum_{i,j} |A_{i,j}|^2)^{1/2}$ is the Euclidean norm of the matrix $\boldsymbol{A}$ (all results have also been rechecked by using the spectral norm giving almost identical results). As the matrix $\boldsymbol{P}(t)$ will be calculated numerically from one very long but finite orbit, it will have statistical error σ_{T} due to a finite number of simulated transitions. In addition, σ will also have a contribution σ_{M} from a systematic error because the process may not be precisely Markovian. We have assumed $\sigma^2 = \sigma_{\mathrm{M}}^2 + \sigma_{\mathrm{T}}^2$ and made an estimate for the statistical error σ_{T} as the square root of the number of average transitions per matrix element n:

$$\sigma_{\mathrm{T}} = c\frac{1}{\sqrt{n}} = c\frac{N}{2}\sqrt{\frac{M_0}{N_0}}, \tag{23}$$

where N_0 is the total number of all transitions between the signatures of order 0, and c is some unspecified numerical constant which has been determined from the numerical data. Its value turned out to be $c \approx 0.7$. Results for the dependence of a systematic error σ_{M} are shown in figure 7. The error $\sigma_{\mathrm{M}}(\tau)$ tends to zero with increasing τ, as expected. Even more interesting is the fact that the error also seems to decrease with increasing N at constant τ. This is interesting, as it means that with increasing N we do not have to keep the fraction of higher-order states small in order for the process to stay Markovian.[2]

Whether a given system can be described as a Markov process can be checked also by calculating the transition matrix $\boldsymbol{P}(t)$ and comparing it with the exponential formula (13) as a function of time. $\boldsymbol{P}(t)$ can be calculated numerically directly from the definition, for instance by using the formula (11). This definition would have a meaning even if the transitions were not Markovian. We then compare the correlation functions between the characteristic functions (17) and the matrix elements of the propagator $\langle S|\exp(\boldsymbol{F}t)|S'\rangle$. These calculations

[1] We have numerically checked that the distribution of Lyapunov exponents is approximately linear, as is typically the case for sufficiently chaotic systems [16].

[2] In such a case, one could bring higher order signatures back and describe a complete hierarchy of transitions between signatures of various orders as a Markov process on 2^N dimensional space.

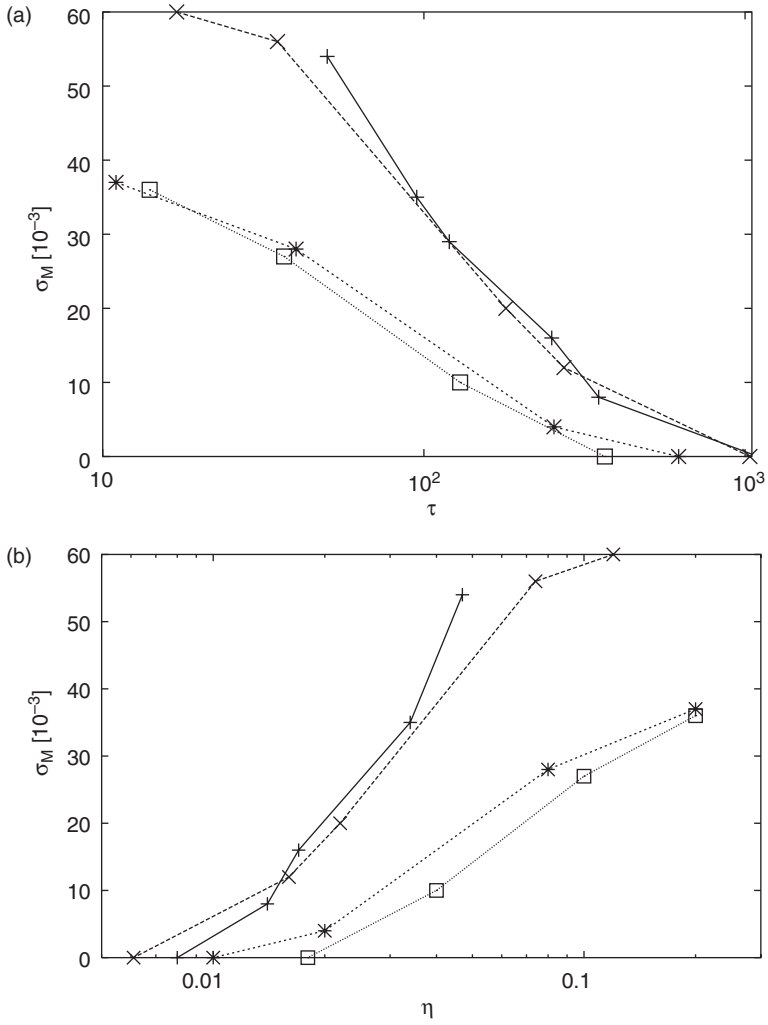

Figure 7. Dependence of σ_M on τ in (*a*) and on $\eta = (\sum_{i=1}^{\infty} t_i)/t_0$ in (*b*). Pluses, crosses, stars and squares are for $N = 6$, 8, 10 and 12, respectively.

should agree only if the flux matrix $\boldsymbol{F}(t) = \log \boldsymbol{P}(t)/t$ were time independent and this would signal that the transitions are described by a Markov process. Numerical results for this test are shown in figure 8. Correlation functions calculated in both ways have been computed for the characteristic function $B_S \equiv |S\rangle$ on the signature $S = 54$ and for the *macroscopic observable* with the vector $w_S = S \bmod 2$, i.e. characteristic function on a union of half of all signatures with the first bit $a_1 = 1$, denoted by $|s1\rangle$. It can be seen from the figure that the autocorrelation function of the observable $|s1\rangle$ begins to fall as $\exp(-\lambda_1 t)$, where λ_1 is the biggest non-trivial eigenvalue of $\boldsymbol{F}$, very early. This is a consequence of relatively large overlap between the macroscopic state $|s1\rangle$ and the eigenstate $|v_1\rangle$ corresponding to the eigenvalue λ_1. We will show in subsection 5.2 that $|\langle s1|v_1\rangle|^2 \sim 1/N$ while $|\langle S|v_1\rangle|^2 \sim 1/M_0$, so $|\langle s1|v_1\rangle|^2 \gg |\langle S|v_1\rangle|^2$ (for $N \gg 1$).

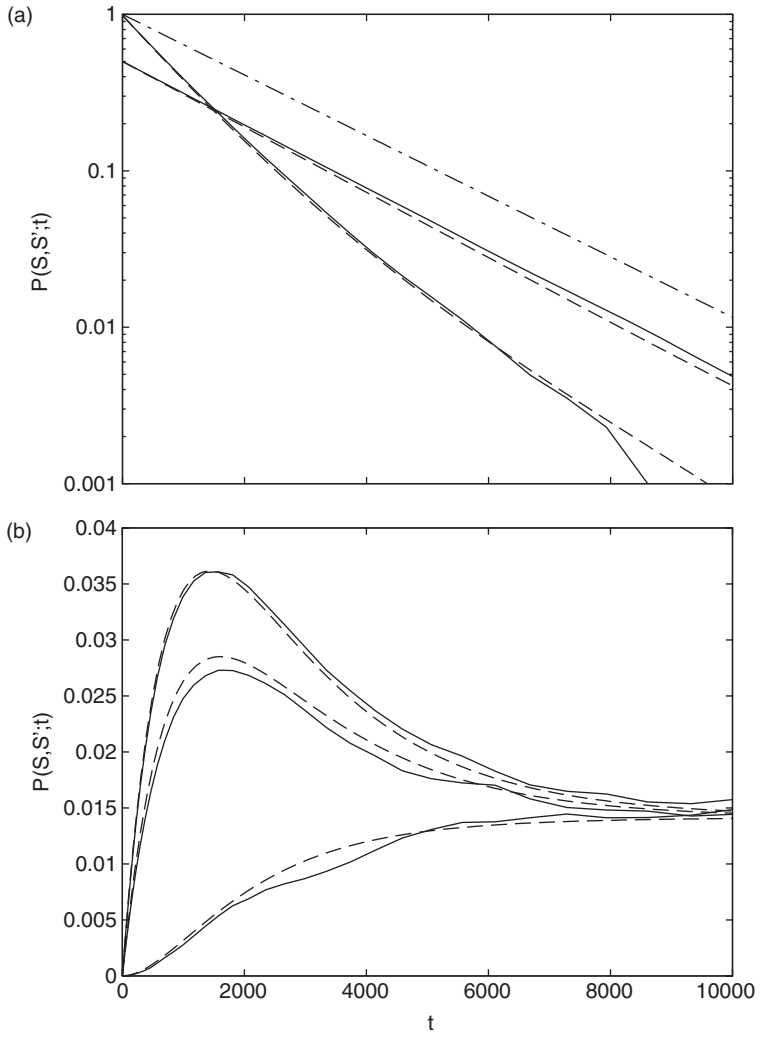

Figure 8. Comparison of the correlation functions calculated from the propagator $\exp(\boldsymbol{F}t)$ (- - - -) and from the directly determined transition matrix $P(S, S'; t)$ (——). (*a*) Autocorrelation functions $S = S'$. (*b*) Cross-correlation functions $S \neq S'$. The bottom pair of curves in (*a*) is for the signature $S = 54$, the middle pair for the one particle state $|s1\rangle$, and the top curve is a simple exponential decay with the biggest non-zero eigenvalue of the matrix $\boldsymbol{F}$. From all correlation functions we have subtracted the equilibrium value which is $P(S, S; t \to \infty) = 1/M_0$ or $1/2$ for the state $|s1\rangle$. (*b*) Correlation functions between the signature $S = 54$ and the signature $S' = 58$, $S' = 116$, and $S' = 135$, from top to bottom, respectively. The chain length and the parameter were $N = 8$, $\alpha = 3.83$, $\tau \sim 1000$.

5. The form and the spectral properties of the flux matrix

Some remarks can be made immediately about the spectrum of $\boldsymbol{F}$. Conservation of probability implies all eigenvalues λ_i to be smaller than or equal to zero. Further, because the system is believed to be ergodic, there should be a non-degenerate constant eigenvector with the corresponding eigenvalue $\lambda_0 = 0$. This is a consequence of the Perron–Frobenius form of the matrix $\boldsymbol{P}$. For finite N, the spectrum of the flux matrix is discrete and the correlation

functions will fall asymptotically as $\exp(-\lambda_1 t)$ where λ_1 is the smallest non-zero eigenvalue. An interesting question is what happens in the thermodynamic limit $N \to \infty$. If there is a spectral gap, we will have an exponential decay, otherwise some anomalous behaviour can occur. The thermodynamical limit has to be defined in such a way as to preserve the Markovian property; this means increasing N while keeping τ or η constant (which enforces increasing α).

5.1. Numerical calculation of the flux matrix

Non-vanishing matrix elements of $\boldsymbol{F}$ are expected only between the signatures that differ only by two bits provided that $t_1/t_0 \ll 1$. In other words, two bits $a_i = 1$ and $a_j = 0$ only switch their position. Such a transition will be called a (bit) jump of length d, where $d = |j - i|$ is the distance between the two bits involved. An example of such a transition has been shown in figure 2. We have numerically calculated complete matrices $\boldsymbol{F}$ for sizes $N = 6, 8, 10$ and 12 and different τ (or α), in order to check the above hypothesis and to obtain some knowledge about the sizes and the structure of matrix elements. The only matrix elements which are really non-vanishing are those of the bit jumps, and what is more, the value of the matrix element depends only on the distance d of the jump and not on the particular signatures involved. This practically means that in addition to the diagonal elements we have only $N/2$ different matrix elements in the flux matrix $\boldsymbol{F}$. This number must be compared to the total number of matrix elements M_0^2 which grows exponentially with N. We have checked this also for the matrices $\boldsymbol{F}$ of sizes up to $N = 30$, but in this case we have compared only the jumps of length d with different number of bits 1 on the sites between the two jump sites. We confirmed that the probability fluxes of jumps depend only on the length d. It is therefore meaningful to introduce dimensionless coefficients c_d which are ratios between the matrix elements of a jump of length d and a jump of length $d = 1$. Therefore, $c_1 \equiv 1$, by definition, and the rest of the $N/2 - 1$ coefficients c_d together with the average transition time τ is all that we need in order to specify the flux matrix $\boldsymbol{F}$ completely. We can write

$$\boldsymbol{F} = \frac{1}{\tau} \frac{2N - 2}{N^2(c_{N/2}/2 + \sum_{d=1}^{N/2-1} c_\mathrm{d})} \boldsymbol{C}, \tag{24}$$

where the matrix $\boldsymbol{C}$ is just a matrix involving the coefficients c_d only. Numerical values of c_d for different N and τ are listed in table 1. It can be seen that for not too big τ (e.g. $\tau = 11$ and $N = 10$) the coefficients c_d decrease monotonically with the distance d. For bigger τ (e.g. $\tau = 621$ and $N = 10$), this dependence ceases to be monotonic but becomes slightly well-shaped with a minimum at around $d \approx N/4$. There also seems to be a general trend that, with increasing N, at a constant fraction $\eta \approx t_1/t_0$, the coefficients c_d all approach 1. This can be explained by the following heuristic argument. To keep the fraction t_1/t_0 of higher-order states constant with increasing N we must increase the barrier height ΔU. As a consequence, the transition time τ increases and correspondingly also the average time $\tau t_1/t_0$ spent in the non-equilibrium intermediate state of order 1 in between the states of order 0. At a constant t_1/t_0, the transition time τ depends approximately exponentially on the chain length N (see figure 4). On the other hand, the relaxation time for the non-equilibrium energy distribution at the moment of transition grows perhaps only linearly with N (inversely proportional to the sound speed), but certainly slower than exponentially. For sufficiently large N, the relaxation time will, therefore, be smaller than the time spent in the intermediate order 1 cell. An initial locally non-equilibrium distribution at the beginning of a jump will, therefore, relax before the transition to the new order 0 state, all of which will therefore be equally probable. Because of this, we can assume that the coefficients c_d will not depend on d in the thermodynamic limit. This hypothesis still needs further verification as the limit of high N could not be tested

Table 1. Dependence of $c_{\rm d}$ on distance d for different τ and N. Errors in $c_{\rm d}$ are smaller than 0.01.

τ	$\eta[10^{-2}]$	c_2	c_3	c_4	c_5	c_6
$N=6$						
50	4.7	0.71	0.64			
360	1.4	0.72	0.66			
1100	0.8	0.73	0.66			
$N=8$						
17	12	0.72	0.61	0.57		
180	2.2	0.76	0.67	0.65		
1030	0.6	0.76	0.71	0.71		
$N=10$						
11	20	0.74	0.61	0.54	0.52	
250	2.0	0.80	0.74	0.76	0.78	
621	1.0	0.82	0.76	0.82	0.86	
$N=12$						
37	10	0.79	0.68	0.63	0.62	0.63
130	4.0	0.81	0.73	0.71	0.76	0.79
366	1.8	0.83	0.76	0.76	0.85	0.92

due to the fast growth of the dimension M_0 with N. Despite that, the numerical results are consistent and point in the right direction (see table 1). We will show now that our flux matrix has a specially appealing form which can be described using a formal connection to a certain Hamiltonian of a quantum spin-1/2 chain. Based on this, we will also deduce the essential spectral properties of the flux matrix.

5.2. Correspondence between the Markov process and the quantum spin chain

We can make the announced correspondence by connecting the eigenvalue problem for the flux matrix $\boldsymbol{F}$ with the eigenvalue problem for the quantum Hamilton operator $\hat{H}$ over M_0-dimensional Hilbert space with the same matrix elements as $\boldsymbol{F}$. This correspondence would generally be of no particular use since the Hamiltonian H does not represent any simple quantum system. In our example of the IFPU chain, this is not the case, since $\boldsymbol{F}$ has a particularly nice and simple form, with non-vanishing elements only between the signatures connected by a bit jump where signatures are sequences of binary bits, 0 and 1. This should immediately remind us of Heisenberg chains of quantum spin-1/2 particles. Let us write the Hamilton function for a one-dimensional ferromagnetic Heisenberg spin chain of length N, with Pauli variables $\sigma_j = (\sigma_j^x, \sigma_j^y, \sigma_j^z)$ and coupling constants $J(d)$:

$$\hat{H} = -\frac{1}{2}\sum_{j,d=1}^{N} J(d)\boldsymbol{\sigma}_j \cdot \boldsymbol{\sigma}_{j+d} = -\frac{1}{2}\sum_{j,d=1}^{N} J(d)\left\{\sigma_j^z\sigma_{j+d}^z + \frac{1}{2}\left(\sigma_j^+\sigma_{j+d}^- + \sigma_j^-\sigma_{j+d}^+\right)\right\}, \tag{25}$$

where periodic boundary condition is assumed to be $\sigma_{N+j} \equiv \sigma_j$ and $J(d) \equiv J(N-d)$, $J(0) \equiv 0$. Operators $\sigma_j^{\pm} = \sigma_j^x \pm \mathrm{i}\sigma_j^y$ are the standard raising and lowering operators. The quantum state of the spin chain, an eigenstate of σ_j^z, will be denoted by the signature $|S\rangle$, with the obvious interpretation. Bit $a_j = 1$ or 0 denotes spin j up or down, respectively. Now we can calculate the matrix elements of the Hamiltonian operator (25). For the off-diagonal elements we get

$$\langle S|\hat{H}|S'\rangle = \begin{cases} -2J(d) & \text{if there is a jump of length } d \text{ connecting } S \text{ and } S', \\ 0 & \text{otherwise.} \end{cases} \tag{26}$$

The diagonal elements are

$$\langle S|\hat{H}|S\rangle = -J(N/2)\left[N/2 - 2s_{N/2}(S)\right] - \sum_{d=1}^{N/2-1} J(d)\,[N - 2s_d(S)], \tag{27}$$

where $s_d(S)$ is a number of different signatures that can be reached from the signature S with a jump of length d. For any signature S we can write an identity

$$\sum_{d=1}^{N/2} s_d(S) = \left(\frac{N}{2}\right)^2. \tag{28}$$

By denoting $s = M_0N^2/(2N-2)$, the following equality is also valid:

$$\sum_{i=1}^{M_0} s_d(S_i) = \begin{cases} s & d = 1, \ldots N/2 - 1, \\ s/2, & d = N/2. \end{cases} \tag{29}$$

The ground state for the ferromagnetic Heisenberg Hamiltonian (25) can be found immediately for any $J(d) > 0$. We have to keep in mind that in our case the Hilbert space is spanned just by M_0 signatures of order 0, and not by all possible signature states as is usual for the quantum spin chains. Order i of the signature is simply an eigenvalue of the S_z component of the total spin, namely $S_z = \sum_j \sigma_j^z/2 = i$. But the operator S_z commutes with the Hamilton function and the Hilbert space is therefore a direct sum of subspaces labelled by eigenvalues of S_z. We choose M_0 dimensional Hilbert subspace with $S_z(= i) = 0$. The ground state denoted by $|0\rangle$ is

$$|0\rangle = \frac{1}{\sqrt{M_0}} \sum_{i=1}^{M_0} |S_i\rangle, \tag{30}$$

with the energy

$$E_0 \equiv \langle 0|\hat{H}|0\rangle = -N\left(\sum_{d=1}^{N/2-1} J(d) + \frac{1}{2}J(N/2)\right). \tag{31}$$

Now that we have the matrix elements of $\hat{H}$ and the ground state, we can see that if we prescribe $J(d)$ to equal c_d multiplied by the constant prefactor in front of the matrix $\boldsymbol{C}$ in the equation for $\boldsymbol{F}$ (24), we can formally write our flux matrix in terms of the Heisenberg spin Hamiltonian (25),

$$\boldsymbol{F} = -\boldsymbol{H} + E_0\boldsymbol{I}. \tag{32}$$

The transition probabilities $P(S, S'; t)$ can now be written as

$$\boldsymbol{P}(t) = \exp(\boldsymbol{F}t) = A(t)\exp(-\beta\boldsymbol{H}), \tag{33}$$

where we wrote $\beta = t$ and $A(t) = \exp(E_0 t)$. The expression for $\boldsymbol{P}$ has the same form as the density operator for the quantum canonical distribution at temperature $1/t$. The time dependence of $\boldsymbol{P}$ is, therefore, the same as the dependence of the canonical distribution on cooling. Understanding the time dynamics of the IFPU model is equivalent to the cooling of the ferromagnetic Heisenberg spin chain or its imaginary-time dynamics. In the limit $t \to \infty$ the matrix elements of $\boldsymbol{P}$ tend to a constant value, $1/M_0$, and in the corresponding Heisenberg spin chain any non-equilibrium distribution relaxes to the ground state $|0\rangle$.

For higher-lying states, we numerically solved the eigenvalue problem for the flux matrix at various τ and sizes up to $N = 12$. One such example of a numerical spectrum is shown in figure 9. We have said that with increasing N, at constant t_1/t_0, we expect coefficients c_d to approach a constant value $c_\mathrm{d} = 1$ independent of d. This case corresponds to the simplest

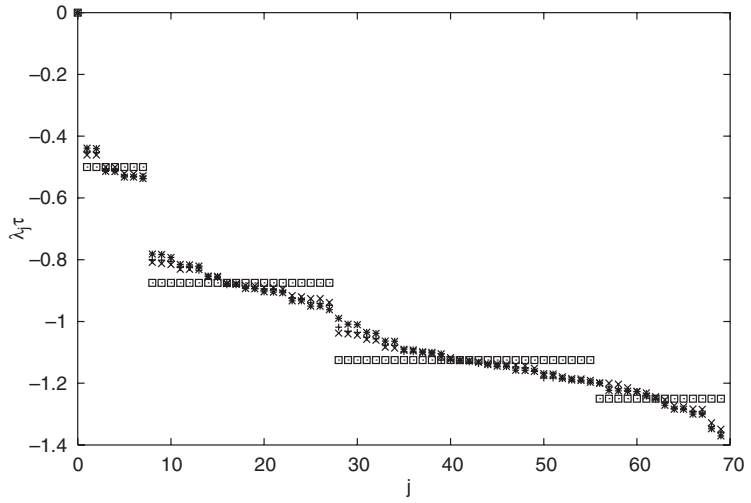

Figure 9. Spectrum of $\boldsymbol{F}$ for $N = 8$ at three different τ values, 17, 180 and 1030, shown with $*$, $+$ and $\times$ respectively. The spectrum in the case $c_{\rm d} \equiv 1$ (35) in also shown with $\square$ for comparison.

Heisenberg spin chain with uniform coupling. Apart from the constant factor the Hamilton function (25) is, in this case, $H = -2\boldsymbol{S}^2 + 3N/2$ and the matrix $\boldsymbol{F}$ reads

$$\boldsymbol{F} = \frac{2}{N^2\tau}\left(2\boldsymbol{S}^2 - \frac{N(N+2)}{2}\boldsymbol{I}\right), \tag{34}$$

where $\boldsymbol{S}^2 = 1/4(\boldsymbol{\sigma}_1 + \cdots + \boldsymbol{\sigma}_N)^2$. Eigenvalues of $\boldsymbol{S}^2$ are $S(S+1)$, where S is the quantum number of the total spin with values from $S = 0, \ldots, N/2$. The Hilbert space is composed of order 0 states with $S_z = 0$. If we denote by λ_j the eigenvalues of operator (34) and by $n(j)$ the corresponding multiplices, we have

$$\begin{aligned} \lambda_j &= -\frac{4j(N+1-j)}{N^2\tau}, \\ n(j) &= \frac{(N+1-2j)N!}{(N+1-j)!(j)!}, \qquad j = 0, \ldots, N/2. \end{aligned} \tag{35}$$

Particularly interesting are the first two eigenvalues λ_0 and λ_1. The largest, non-degenerate eigenvalue $\lambda_0 = 0$ belongs to the ground state $|0\rangle$. The largest non-trivial eigenvalue is $\lambda_1 = -4/N\tau$ with the multiplicity $n(1) = N - 1$. In the thermodynamic limit and keeping τ constant, it tends to zero as $1/N$. The correlation functions, therefore, decay *slower than exponential* in the thermodynamic limit. From figures 9 and 10 it can also be deduced that with increasing τ the spectrum is indeed approaching the spectrum for $c_{\rm d} \equiv 1$ (35), as predicted. In addition, the eigenvalue λ_1 seems to be monotonically approaching the limiting case ($c_{\rm d} \equiv 1$) from above. We can therefore conclude by observation that the correlation functions of observables which can be spanned by $|S\rangle$ decay slower than $\exp(-4t/N\tau)$.

Now that we expect the spectrum to be close to the one for $c_{\rm d} \equiv 1$ we can explain the decay of the correlation functions for *one particle state* $|s1\rangle$ and the *one signature state* $|S\rangle$ in figure 8. The state vector for $|S\rangle$ has only one component different from 0. Eigenvector $|v_1\rangle$ corresponding to the eigenvalue λ_1 has, on the other hand, all components approximately of the same order, i.e. $1/\sqrt{M_0}$. The square of the scalar product is, therefore, $|\langle S|v_1\rangle|^2 \sim 1/M_0$. The one-particle state $|s1\rangle$ is proportional to $|s1\rangle \sim \sigma_1^+\sigma_1^-|0\rangle$. Because we act on the state $|0\rangle$ with the eigenvalue $S = N/2$ with the operator $\sigma_1^+\sigma_1^-$, we can decompose the state $|s1\rangle$ as

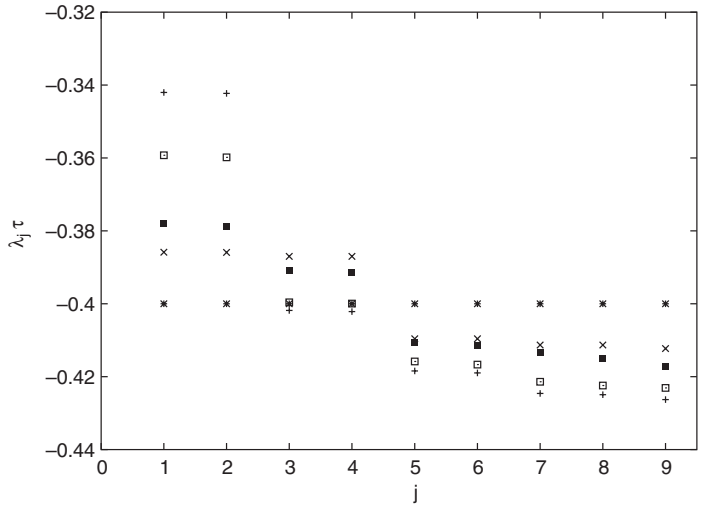

Figure 10. Enlarged first multiplets for $N = 10$ and $\tau = 11, 40, 250$ and 620 are shown using +, □, ■ and ×, respectively. The referential degenerate set of first $N - 1$ eigenvalues at $c_d \equiv 1$ is also shown (∗).

a linear combination of states with the eigenvalues $S = N/2$ and $S = N/2 - 1$. State $|s1\rangle$ can therefore be written as a sum of N states, one of which is also $|v_1\rangle$. If we assume all the expansion coefficients to be of the same order, we immediately obtain $|\langle s1|v_1\rangle|^2 \sim 1/N$.

6. Discussion and conclusion

We divide the phase space of a N-body Hamiltonian, namely the IFPU model, into 2^N cells that are uniquely tagged by a binary number, called a signature (3). Signatures are *ordered* according to the absolute difference in the number of particle pairs/bits in the left/0 and right/1 potential well. For a sufficiently high potential barrier, an approximate Markovian description on space spanned by order 0 signatures is possible. The accuracy of the Markovian property has been checked numerically to be increasing with increasing chain length N at a constant fraction of higher-order states. In the flux matrix $\boldsymbol{F}$, we have non-vanishing matrix elements only between the signatures connected by an exchange of a pair of bits. This makes possible the formal correspondence between the IFPU and ferromagnetic Heisenberg quantum spin-1/2 chains. Understanding the time dependence of a Markov transition matrix is equivalent to cooling or the imaginary-time dynamics of a quantum spin chain. If we increase the chain length N at a fixed fraction of higher-order states η, the transition rates are expected to become independent of a jump length d. Such a trend is confirmed by numerically calculated matrices $\boldsymbol{F}$. In this type of thermodynamic limit, exact eigenvalues of a flux matrix can be obtained explicitly. The largest non-trivial eigenvalue in this case is $\lambda_1 = -4/N\tau$. There is also numerical evidence that the largest non-trivial eigenvalue in a general case (for a non-constant transition rate, e.g. keeping τ constant) is strictly larger than $-4/N\tau$. Therefore, the correlation functions of the observables which can be spanned by functions $|S\rangle$ decay asymptotically slower than $\exp(-4t/N\tau)$. From our analysis, we cannot make any definite predictions regarding possible power-law decay in this limit as is, for instance, the case for the Lorentz gas [17].

Unfortunately, these results do not imply directly the behaviour of more general correlation functions, such as current–current correlation which is needed in order to understand the

transport properties. We have made some numerical calculations of current–current time correlation functions of the IFPU chain for different sizes N and different parameters. As expected, the decay of the correlations for observables that vary on timescales smaller than τ (e.g. current) is faster than the decay of correlation functions spanned by the piecewise constant basis $|S\rangle$. Transition from the algebraic (anomalous conductivity) to the exponential (normal conductivity) decay of the current autocorrelation function occurs rather abruptly at $\alpha \approx 3$ (for $N \geqslant 20$).

Finally, although we suggested several interesting properties of the above model, we must admit that most of our conclusions are based on numerical evidence. Therefore, we believe that it should be a challenging and not impossible future task to try to provide more rigorous justifications (and perhaps proofs) of our results. Establishing a rigorous asymptotic Markovian property would enable one to systematically code and enumerate all the many-body (unstable, hyperbolic) periodic orbits and to use them explicitly in a classical or semiclassical *trace formulae*, for example, to calculate the transport coefficients directly. We feel that the IFPU chain may become a useful toy model of a *chaotic field theory* [18].

Acknowledgments

Financial support by the Ministry of Science and Technology of Slovenia is gratefully acknowledged.

References

[1] Fermi E, Pasta J and Ulam S 1955 *Los Alamos Report* no LA-1940, reprinted in Fermi E 1965 *Collected Papers* Vol II (Chicago: University of Chicago Press) p 978
[2] Ford J 1992 The Fermi–Pasta–Ulam problem: paradox turns discovery *Phys. Rep.* **213** 271–310
[3] Izrailev F M and Chirikov B V 1966 *Sov. Phys.–Dokl.* **11** 30
[4] Shepelyansky D L 1997 Low-energy chaos in the Fermi–Pasta–Ulam problem *Nonlinearity* **10** 1331–8
[5] Lepri S, Livi R and Politi A 1997 Heat conduction in chains of nonlinear oscillators *Phys. Rev. Lett.* **78** 1896–9
Lepri S, Livi R and Politi A 1998 Energy transport in anharmonic lattices close and far from equilibrium *Physica* D **119** 140–7
[6] Hatano T 1999 Heat conduction in the diatomic Toda lattice revisited *Phys. Rev.* E **59** R1–4
[7] Fillipov A, Hu B, Li B and Zeltser A 1998 Energy transport between two attractors connected by a Fermi–Pasta–Ulam chain *J. Phys. A: Math. Gen.* **31** 7719–28
[8] Lepri S, Livi R and Politi A 1998 On the anomalous thermal conductivity in one-dimensional lattices *Europhys. Lett.* **43** 271–6
[9] Giardina C, Livi R, Politi A and Vassalli M 2000 Finite thermal conductivity in 1D lattices *Phys. Rev. Lett.* **84** 2144–7
[10] Prosen T and Campbell D K 2000 Momentum conservation implies anomalous energy transport in 1D classical lattices *Phys. Rev. Lett.* **84** 2857–60
[11] Konishi T 1989 Relaxation and diffusion in hamiltonian systems with many degrees of freedom *Prog. Theor. Phys. Supp.* **98** 19–35
[12] Gallavotti C and Cohen E G D 1995 Dynamical ensembles in non-equilibrium statistical mechanics *Phys. Rev. Lett* **74** 2694–7
Gallavotti C and Cohen E G D 1995 Dynamical ensembles in stationary states *J. Stat. Phys.* **80** 931–70
[13] McLachlan R and Atela P 1992 The accuracy of symplectic integrators *Nonlinearity* **5** 541–62
[14] Robnik M, Dobnikar J, Rapisarda A, Prosen T and Petkovšek M 1997 New universal aspects of diffusion in strongly chaotic systems *J. Phys.* A*: Math. Gen.* **30** L803–13
[15] Gaspard P 1998 *Chaos, Scattering, and Statistical Mechanics* (Cambridge: Cambridge University Press)
[16] Livi R, Politi A, Ruffo A and Vulpiani A 1987 Lyapunov exponents in high-dimensional symplectic dynamics *J. Stat. Phys.* **46** 147–60
[17] van Beijeren H 1982 Transport properties of stochastics Lorentz models *Rev. Mod. Phys.* **54** 195–234
[18] Cvitanović P 2000 Chaotic field theory: a sketch *Physica* A **288** 61–80